

# Microwave assisted synthesis of CdS nanoparticles and their size evolution

I. A. López, A. Vázquez, and I. Gómez\*

*Universidad Autónoma de Nuevo León, Facultad de Ciencias Químicas, Laboratorio de Materiales I,  
Av. Universidad, Cd. Universitaria 66451, San Nicolás de los Garza, Nuevo León, Mexico.*

\*e-mail: idaliagomezmx@yahoo.com.mx

Received 2 May 2012; accepted 7 December 2012

The study of the size evolution of CdS nanoparticles in aqueous dispersion is presented in this paper. The sodium citrate was employed as stabilizer of CdS nanoparticles synthesized by microwave assisted synthesis. Analysis of this study was carried out by UV-Vis spectrophotometry, by comparison of the band gap energy using theoretical and empirical models. Results obtained show that the synthesis conditions produce CdS nanoparticles with diameters below of 6 nm, which remains stabilized by at least 14 days. These characteristics were confirmed by transmission electron microscopy. The X-ray diffraction pattern confirms cubic phase of the CdS nanoparticles.

*Keywords:* Microwaves; cadmium sulfide; nanoparticles; stabilization

PACS: 81.07.-b

## 1. Introduction

Over the past few decades, the scientific activity has been focused on the study and development of nanomaterials, especially nanosemiconductors. These materials are important not only because of their unconventional properties which depends on dimensionality, but also because these materials can be useful for many technological applications such as solar cells [1], biologic systems [2], photocatalytic processes [3], optoelectronic devices [4], among others.

CdS is one of the most important II-VI semiconductors. It is an important semiconductor with a direct-band transition and with a band gap ( $E_g$ ) of 2.53 eV [5]. CdS has important optoelectronic applications for laser light emitting diodes [6] and optical devices based on nonlinear properties [7].

There are numerous reports on the synthesis of CdS nanoparticles, such as sol-gel [8,9], chemical vapor deposition [10,11], solvothermal [12,13] and spray pyrolysis [14,15]. However a rapid and inexpensive method is the microwave (MW) assisted synthesis [16-18]. In general, MW assisted synthesis routes offer advantages like short reaction times and high energy efficiency because the radiation is directly converted to thermal energy and there is not thermal gradients [19], besides, it can be easily adapted to the industrial scale.

One of the most important goals of materials chemistry is the control of size and the nanoparticles stability. Since the nanoparticles are thermodynamically unstable, an agglomeration effect and then a consequent crystal growth have placed. To avoid this consequence, the nanoparticles are stabilized with organic systems that “enveloped them” and obstruct their agglomeration and consequently their growth. Some compounds have been utilized with this purpose, like polyvinyl alcohol [20], thiophenol [21] and sodium citrate [22]. However, due to toxicity and environmental impact sodium citrate is preferred as stabilizer of nanoparticles.

In this work we present the results of the study of stabilization of CdS nanoparticles in aqueous dispersion using

sodium citrate as stabilizer. The CdS dispersion was synthesized by MW heating in a conventional MW oven at pH 8. The MW heating was chosen in order to avoid thermal gradients present in the conventional heating. The size of CdS nanoparticles was estimated through UV-Vis spectrophotometry, by comparison of the  $E_g$  values with an empirical and a theoretical model.

## 2. Experimental Section

All the reactants and solvents used in this work were of analytical grade and used without any further purification. The dispersions obtained were characterized by means of UV-Vis spectroscopy, with a Perkin Elmer Lambda 12 spectrophotometer. Luminescence analysis was carried out in a Perkin Elmer LS 55 spectrophotometer, and a Perkin Elmer Spectrum-One spectrometer was employed for the Fourier transform infrared (FT-IR) analysis. The transmission electron microscopy (TEM) images were recorded on a JEOL 2010 microscope. X-ray diffraction (XRD) pattern was carried out in a Siemens D5000 ( $\lambda = 1.5418 \text{ \AA}$ ).

Two solutions of concentration 30 mM were prepared, first one of thioacetamide (TAA) and second one of cadmium chloride. These solutions were mixed in stoichiometric ratios, the resulting solution was diluted to 50 mL with a 2 mM sodium citrate solution and the pH was fixed at 8 with a KOH solution. Finally, the reaction mixture was heated in a conventional MW oven LG-intelowave at 2.45 GHz and 1650 W of nominal power, for 60 seconds. The resulting CdS nanoparticles dispersions were analyzed during 2 weeks by UV-Vis and luminescence spectrophotometry.

## 3. Results and Discussion

Figure 1 shows the absorbance spectra for CdS nanoparticles dispersions, at different times after the synthesis procedure. The  $E_g$  values were evaluated by fitting a straight line through

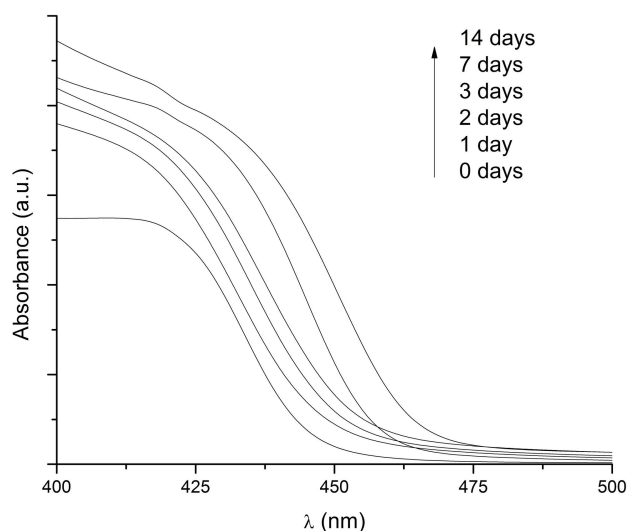


FIGURE 1. UV-Vis spectra of the CdS nanoparticles early synthesized and after several days.

a lineal portion of the curve to zero absorbance, and the values of wavelength were converted to energy in eV units. Values founded were in the ranges from 2.77 to 2.67 eV. The  $E_g$  value reported for the CdS in bulk is 2.53 eV. Effects of quantum confinement are evident in all conditions, which suggest that particles of CdS are in nanometric scale. Besides a red shift is observed after some days of the synthesis, which means that the particles are growing.

The wavelength values corresponding to the  $E_g$  were employed for particle size determination, by comparison with two different models. Yu model [23] is an empirical relationship between the wavelength ( $\lambda$ ) values corresponding to the  $E_g$  and the particle diameter ( $D$ ) expressed as:

$$D = -6.6521 \times 10^{-8} \lambda^3 + 1.9557 \times 10^{-4} \lambda^2 - 9.2352 \times 10^{-2} \lambda + 13.29 \quad (1)$$

and Brus model [24] is a theoretical model based on quantum mechanics known as the effective mass approximation. This model expresses a relationship between the  $E_g$  energy and the particle radius ( $r$ ) described by the following equation:

$$\Delta E = \frac{\hbar^2 \pi^2}{2r^2} \left( \frac{1}{m_e} + \frac{1}{m_h} \right) - \frac{1.8e^2}{r\epsilon} \quad (2)$$

where  $e$  is the electron charge,  $\hbar$  is the reduced plank constant,  $\epsilon$  is the dielectric constant,  $m_e$  and  $m_h$  are the reduced masses of the electrons and holes, respectively.

Figure 2 shows the particle size values estimated under both models. Particle diameters are from 4.5 to 6 nm. Three different stages can be appreciated; the first of these stages shows an accelerated growth in the 4 days after synthesis. After that a stabilization stage was presented, during about 2 days and finally a third stage, with an accelerated growth, was observed. This unusual behavior could be attributed to stages of stabilization-destabilization caused by addition of monomers (*i.e.*, CdS molecules) to the particle surface. When

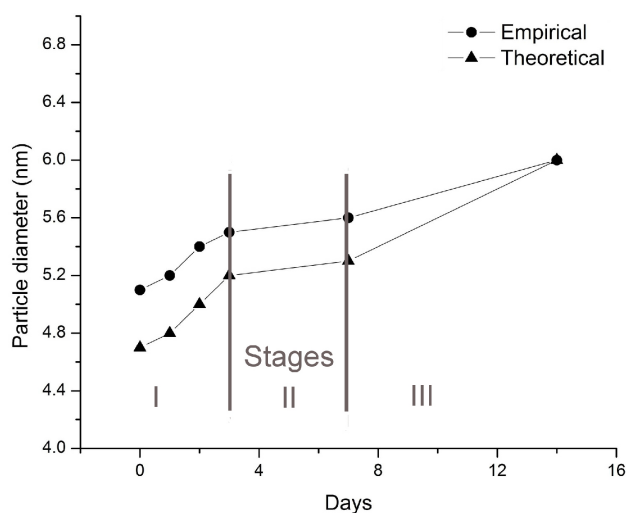


FIGURE 2. Particle size values estimated by an empirical and a theoretical model.

the external layer is completed the particle is stable, but when a monomer is added a new external layer is not completed so the particle is not stable and a rapid addition of monomers occurs to stabilize the particle.

A difference between the two models can be appreciated, probably due to the theoretical model considers only particles with the calculated diameter, while the empirical model assumes that the particle diameter is the average diameter of the actually particle size distribution. Besides, the Eq. 2 is an analytical approximation for the lowest eigenvalue using the model Hamiltonian for the cluster's lowest excited state. For this approximation smaller terms were neglected.

TEM images of the particles synthesized under the conditions described at 0 days of growth are shown in Fig. 3. Particles with diameter around 5 nm are observed in Fig. 3 a). The electron diffraction pattern shown in Fig. 3 b) is in concordance with a cubic phase corresponding to hawleyite (JCPDS 10-454). Atomic planes can be observed in Fig. 3 c) with an interplanar distance of 3.35 Å. This is in good agreement with the distance between planes (111) in hawleyite which is

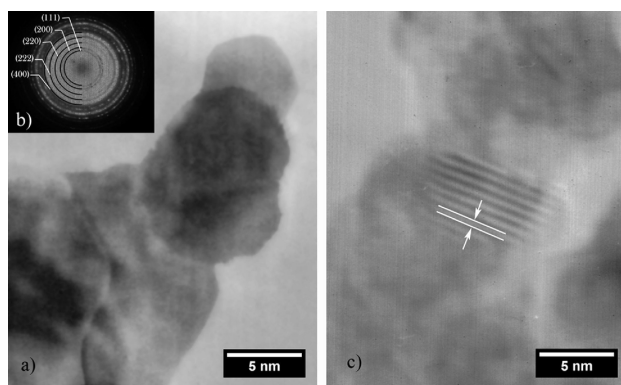


FIGURE 3. TEM images of the CdS nanoparticles early synthesized.

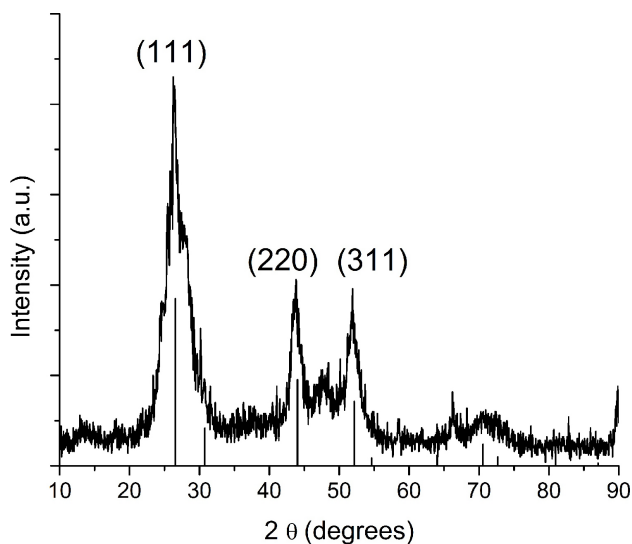


FIGURE 4. XRD pattern of the CdS nanoparticles.

3.43 Å. This difference can be attributed to distortions of the lattice due to the nanometric particle size. TEM images confirm that the empirical model represents more closely the phenomenon.

In Fig. 4, the XRD pattern of CdS nanoparticles shows broad peaks indicating nanometric dimensions of the crystals. The peaks in the XRD pattern are indexed according to the JCPDS data of the cubic structure of CdS (10-454). The XRD peaks in the pattern at 26.3°, 43.8° and 51.9° correspond to the crystal planes (111), (220) and (311), respectively, which agree well with the obtained by electron diffraction.

To describe the growth rate of CdS nanoparticles, we can assume that the growth is controlled by diffusion of monomer passing through a spherical surface within the diffusion layer, epitaxial attachment is negligible. Coarsening processes involve the growth of larger crystals at the expense of smaller crystals and are governed by capillary effects [25]. Since the chemical potential of a particle increases with decreasing particle size, the equilibrium solute concentration,  $c_r$ , for a small particle is much higher than that for a large particle, as described by the Gibbs-Thompson equation:

$$c_r = c_\infty \exp\left(\frac{2\gamma V_m}{rRT}\right) \quad (3)$$

where  $c_\infty$  is the equilibrium concentration for a flat surface (*i.e.*, the bulk solubility),  $\gamma$  is the surface energy,  $V_m$  is the molar volume,  $R$  is the gas constant,  $T$  is the temperature, and  $r$  is the particle radius.

The rate law for this process, derived by Lifshitz, Sloyozov [26], and Wagner [27] (known as LSW theory), is obtained by inserting the Gibbs-Thompson equation into Fick's first law and solving to obtain the dependence of particle size on time. It is given by:

$$r^3 = Kt + r_0^3 \quad (4)$$

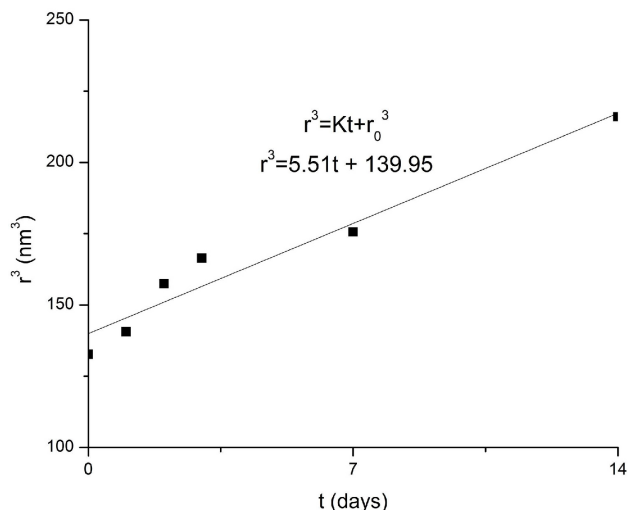


FIGURE 5. Particle radius versus time curve from Fig. 2 plotted as  $r^3$  versus time.

where  $r$  is the average particle radius,  $r_0$  is the average initial particle radius, and  $t$  is time. Some reports [28,29] show the good correspondence of this model with experimental results for oxide semiconductor nanoparticles. The plot  $r^3$  vs  $t$  for CdS Np's is shown in Fig. 5. A square correlation factor  $R^2$  of 0.9359 was obtained. Low linearity of this model could

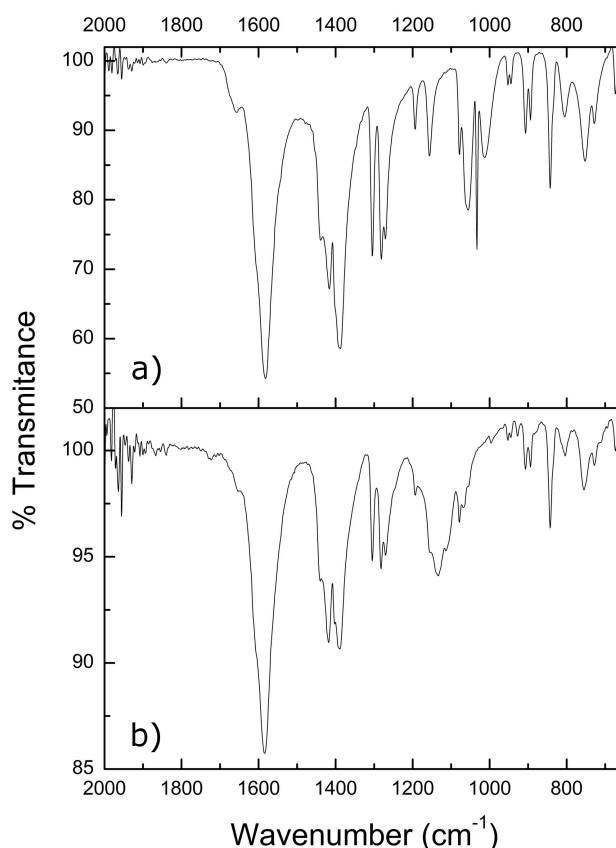


FIGURE 6. FT-IR spectra of the a) sodium citrate and b) CdS nanoparticles early synthesized.

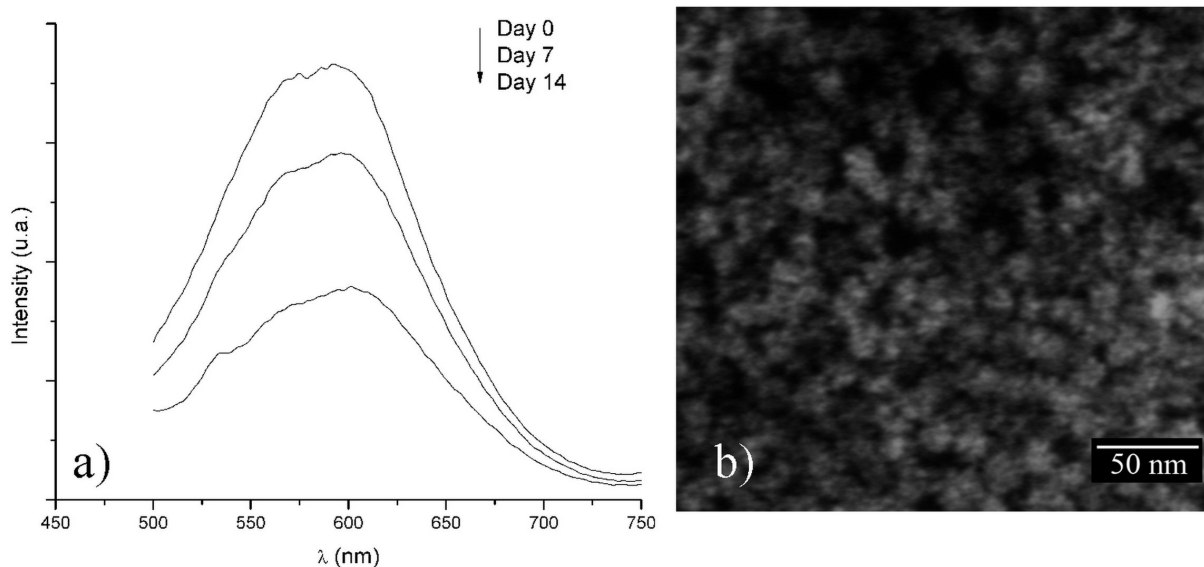


FIGURE 7. a) Luminescence spectra of the CdS nanoparticles early synthesized and after several days. b) SEM image of particles 14 days after the synthesis.

be explained by the non-adequate expansion of the Gibbs-Thompson equation, which is important in very small particles systems, as suggest Talapin and coworkers [30]. However, the results obtained in this work can help to understand the growth mechanisms of particles with this size range.

Dispersions were dried at room temperature, and the resulting solids were analyzed by FT-IR to determine the citrate ions adsorbed on the particles. Fig. 6 a) shows the FT-IR spectra of the sodium citrate, and Fig. 6 b) the corresponding spectra for the CdS nanoparticles. This figure confirms the presence of the citrate ions adsorbed on the CdS nanoparticles. The band observed at  $1582\text{ cm}^{-1}$  is assigned to the asymmetrical stretching of the citrate ion carboxylates.

The luminescence spectra of the different experimental conditions are shown in Fig. 7 a). All samples were excited at 390 nm. A broad emission peak near the 600 nm was observed, corresponding to a yellow-red color. This band can be ascribed to two different phenomena, first one related to the transition of bound electrons from surface states to valence band, and the second one attributed to the transition of Cd-interstitial donors to valence band [31]. Besides, Intensity of the luminescence was decreased in roughly 20 % after 7 days of the synthesis, and in 50 % after 14 days. This fact cannot be explained entirely by the Np's growth, because the difference between the particle radius is only 1 nm. Sergiel

and coworkers found that the optical properties of CdS Np's stabilized with sugars do not change after several days [32]. In our case, the decrease of the luminescence intensity could be attributed to particles agglomeration, and not to particles growth. It is possible that the adsorbed citrate ion onto one particle interacts with that of another particle and forms hydrogen bonds promoting the particles agglomeration. This agglomeration can conduce to non-radiative relaxation. Figure 7 b) shows a SEM image of particles 14 days after the synthesis. Agglomerates of around 20 nm can be observed.

#### 4. Conclusions

MW assisted synthesis of CdS nanoparticles was successfully carry out by experimental conditions early described. CdS nanoparticles with an average diameter around 5 nm, and cubic phase, were obtained using sodium citrate as stabilizer. Size evolution of these particles was monitored through UV-Vis by fitting the  $E_g$  wavelength values to two empirical and theoretical models. The growth of CdS nanoparticles is controlled by diffusion. According with TEM analysis the theoretical model is more appropriated to describe this phenomenon. The particles remain under the 6 nm of diameter by at least 14 days. Nevertheless, the luminescence intensity decreases 50 %, probably due to the particles agglomeration.

1. Y. Hao, Y. Cao, B. Sun, Y. Li, Y. Zhang, and D. Xu, *Sol. Energy Mater. Sol. Cells* **101** (2012) 107.
2. G. Wei, M. Yan, L. Ma, and H. Zhang, *Spectrochim. Acta A* **85** (2012) 288.
3. L. Ge and J. Liu, *Mater. Lett.* **65** (2011) 1828.
4. Y. Xi, C. Hu, C. Zheng, H. Zhang, R. Yang, and Y. Tian, *Mater. Res. Bull.* **45** (2010) 1476.
5. T. Trindade, P. O'Brien, and N.L. Pickett, *Chem. Mater.* **13** (2001) 3843.

6. J. Kim, Y. Kim, and H. Yang, *Mater. Lett.* **63** (2009) 614.
7. M. Feng, Y. Chen, L. Gu, N. He, J. Bai, Y. Lin, and H. Zhan, *Eur. Polym. J.* **45** (2009) 1058.
8. N.V. Hullavarad, and S.S. Hullavarad, *Photonics Nanostruct* **5** (2007) 156.
9. S.M. Reda, *Acta Materialia* **56** (2008) 259.
10. T. Zhai, Z. Gu, H. Zhong, Y. Dong, Y. Ma, H. Fu, Y. Li, and J. Yao, *Cryst. Growth Des.* **7** (2007) 488.
11. B.J.K. Dongre, V. Nogriya, and M. Ramrakhiani, *Appl. Surf. Sci.* **255** (2009) 6115.
12. A. Phuruangrat, T. Thongtem, and S. Thongtem, *Mater. Lett.* **63** (2009) 1538.
13. A. Tang, F. Teng, Y. Hou, Y. Wang, F. Tan, S. Qu, and Z. Wang, *Appl. Phys. Lett.* **96** (2010) 163112.
14. S.J. Ikhmayies and R.N. Ahmad-Bitar, *Appl. Surf. Sci.* **255** (2009) 8470.
15. N. Badera, B. Godbole, S.B. Srivastava, P.N. Vishwakarma, L.S. Chandra, D. Jain, M. Gangrade, T. Shripathi, V.G. Sathe, and V. Ganesan, *Appl. Surf. Sci.* **254** (2008) 7042.
16. E. Caponetti, D.C. Martino, M. Leone, L. Pedone, M.L. Saladino, and V. Vetri, *J. Colloid Interface Sci.* **304** (2006) 413.
17. T. Serrano, I. Gómez, R. Colás, and J. Cavazos, *Colloids Surfaces A. Physicochem. Eng. Aspects* **338** (2009) 20.
18. R. Amutha, M. Muruganandham, G.J. Lee, and J.J. Wu, *J. Nanosci. Nanotechnol.* **11** (2011) 7940.
19. S. Das, A.K. Mukhopadhyay, S. Datta, and D. Basu, *Bull. Mater. Sci.* **32** (2009) 1.
20. H. Wang, P. Fang, Z. Chen, and S. Wang, *Appl. Surf. Sci.* **253** (2007) 8495.
21. M. Pattabi and B.S. Amma, *Sol. Energy Mater Sol. Cells* **90** (2006) 2377.
22. D. Philip, *Physica E* **41** (2009) 1727.
23. W.W. Yu, L. Qu, W. Guo, and X. Peng, *Chem. Mater.* **15** (2003) 2854.
24. L. Brus, *J. Phys. Chem.* **90** (1986) 2555.
25. Y. De Smet, L. Deriemaeker, and R. Finsy, *Langmuir* **13** (1997) 6884.
26. I.M. Lifshitz and V.V. Slyozov, **19** (1961) 35.
27. C. Wagner, and Z. Elektrochem, *Ber. Bunsenges Phys. Chem.* **65** (1961) 581.
28. Z. Hu, D.J. Escamilla-Ramírez, B.E. Heredia Cervera, G. Oskam, and P.C. Searson, *J. Phys. Chem. B* **109** (2005) 11209.
29. Z. Hu, G. Oskam, R.L. Penn, N. Pesika, and P.C. Searson, *J. Phys. Chem. B* **107** (2003) 3124.
30. D.V. Talapin, A.L. Rogach, M. Haase, and H. Weller, *J. Phys. Chem. B* **105** (2001) 12278.
31. C.T. Tsai, D.S. Chuu, G.L. Chen, and S.L. Yang, *J. Appl. Phys.* **79** (1996) 9105.
32. I. Sergiel, A. Mirończuk, J.J. Koziol, and A. Defort, *Acta Physica Polonica A* **116** (2009) S-166.